J Biol Inorg Chem (2008) 13:449–459
DOI 10.1007/s00775-007-0338-3

ORIGINAL PAPER

Melanoma targeting with α-melanocyte stimulating hormone analogs labeled with *fac*-[^{99m}Tc(CO)$_3$]$^+$: effect of cyclization on tumor-seeking properties

Paula D. Raposinho · Catarina Xavier · João D. G. Correia · Soraia Falcão · Paula Gomes · Isabel Santos

Received: 20 September 2007 / Accepted: 8 December 2007 / Published online: 8 January 2008

Abstract Early detection of primary melanoma tumors is essential because there is no effective treatment for metastatic melanoma. Several linear and cyclic radiolabeled α-melanocyte stimulating hormone (α-MSH) analogs have been proposed to target the melanocortin type 1 receptor (MC1R) overexpressed in melanoma. The compact structure of a rhenium-cyclized α-MSH analog (Re-CCMSH) significantly enhanced its in vivo tumor uptake and retention. Melanotan II (MT-II), a cyclic lactam analog of α-MSH (Ac-Nle-*cyclo*[Asp-His-DPhe-Arg-Trp-Lys]-NH_2]), is a very potent and stable agonist peptide largely used in the characterization of melanocortin receptors. Taking advantage of the superior biological features associated with the MT-II cyclic peptide, we assessed the effect of lactam-based cyclization on the tumor-seeking properties of α-MSH analogs by comparing the pharmacokinetics profile of the ^{99m}Tc-labeled cyclic peptide βAla-Nle-*cyclo*[Asp-His-D-Phe-Arg-Trp-Lys]-NH_2 with that of the linear analog βAla-Nle-Asp-His-DPhe-Arg-Trp-Lys-NH_2 in melanoma-bearing mice. We have synthesized and coupled the linear and cyclic peptides to a bifunctional chelator containing a pyrazolyl-diamine backbone (pz) through the amino group of βAla, and the resulting pz–peptide conjugates were reacted with the *fac*-[^{99m}Tc(CO)$_3$]$^+$ moiety. The ^{99m}Tc(CO)$_3$-labeled conjugates were obtained in high yield, high specific activity, and high radiochemical purity. The cyclic ^{99m}Tc(CO)$_3$-labeled conjugate presents a remarkable internalization (87.1% of receptor-bound tracer and 50.5% of total applied activity, after 6 h at 37 °C) and cellular retention (only 24.7% released from the cells after 5 h) in murine melanoma B16F1 cells. A significant tumor uptake and retention was obtained in melanoma-bearing C57BL6 mice for the cyclic radioconjugate [9.26 ± 0.83 and 11.31 ± 1.83% ID/g at 1 and 4 h after injection, respectively]. The linear ^{99m}Tc(CO)$_3$-pz–peptide presented lower values for both cellular internalization and tumor uptake. Receptor blocking studies with the potent (Nle^4,DPhe^7)-αMSH agonist demonstrated the specificity of the radioconjugates to MC1R (74.8 and 44.5% reduction of tumor uptake at 4 h after injection for cyclic and linear radioconjugates, respectively).

Keywords Melanoma imaging · α-Melanocyte stimulating hormone · Melanocortin type 1 receptor · Technetium-99m · Radiolabeled peptide

P. D. Raposinho · C. Xavier · J. D. G. Correia · I. Santos (✉)
Departamento de Química,
ITN, Estrada Nacional 10,
2686-953 Sacavém, Portugal
e-mail: isantos@itn.pt

S. Falcão · P. Gomes
Centro de Investigação em Química da Universidade do Porto,
Departamento de Química,
Faculdade de Ciências,
Universidade do Porto,
R. Campo Alegre 687, 4169-007 Porto, Portugal

Abbreviations

αMSH	α-Melanocyte stimulating hormone
Boc	*tert*-Butoxycarbonyl
BSA	Bovine serum albumin
DMEM	Dulbecco's modified Eagle's medium
DOTA	1,4,7,10-Tetraazacyclododecane-1,4,7,10-tetraacetic acid
ESI-MS	Electrospray ionization mass spectrometry
^{18}F-FDG	Fluoro-2-deoxyglucose
Fmoc	9-Fluorenylmethoxycarbonyl

HPLC	High-performance liquid chromatography
ID	Injected dose
MC1R	Melanocortin type 1 receptor
MEM	Modified Eagle's medium
MT-II	Melanotan II
NAPamide	[Ac–Nle^4,Asp^5,DPhe^7]–αMSH$_{4–11}$
NDP-MSH	(Nle^4,DPhe^7)-αMSH
PBS	Phosphate-bufered saline
pz	Tridentate ligand containing a pyrazolyl-diamine backbone
RP	Reversed phase
TBTU	*O*-(Benzotriazol-1-yl)-*N*,*N*,*N*′,*N*′-tetramethyluronium tetrafluoroborate
TFA	Trifluoroacetic acid
TLC	Thin-layer chromatography

Introduction

The incidence and mortality rates of cutaneous melanoma are still increasing in most western countries. Early detection of primary melanoma tumors is essential, since the current treatments do not enhance substantially patient survival once metastasis has occurred [1]. Fluoro-2-deoxyglucose (^{18}F-FDG), the most widely used positron-emitter radiopharmaceutical, is limited in detecting melanoma tumors with small foci [2], and some melanoma cells are undetectable with ^{18}F-FDG because they use substrates other than glucose as an energy source [3]. Therefore, development of new melanoma-specific radiopharmaceuticals for imaging or internal radiotherapy is a subject of great interest and intense research. It has been reported that most murine and human melanoma metastasis bear upregulated α-melanocyte stimulating hormone (α-MSH) receptors, namely, the melanocortin type 1 receptor (MC1R) [4–6]. Since radiopeptides have proven their superior usefulness as radioactive probes for cancer diagnosis and internal radiotherapy, a significant research effort has been directed to the development of radiolabeled α-MSH analogs for diagnosis and treatment of melanoma [7–23]. The tridecapeptide α-MSH, the most potent naturally occurring melanotropic peptide and the most active peptide of MC1R [24], has a short half-life in humans, as do many other endogenous peptides (Table 1). The minimal sequence required for biological activity was determined by structure–bioactivity studies to be His-Phe-Arg-Trp, and the replacement of Met^4 and Phe^7 by Nle and DPhe, respectively, led to the more potent (Nle^4,DPhe^7)–αMSH (NDP-MSH) analog (Table 1), which is enzymatically stable and has a longer half-life [25].

Introduction of a cyclic constraint in a lead peptide may restrict the flexibility and favor peptide–receptor interactions, and is an effective way of generating ligands with enhanced potency, receptor selectivity, and enzymatic stability [25]. The concept of side chain to side chain cyclization of melanocortin peptides has been successfully applied, namely, in the case of Ac–[Cys^4,Cys^{10}]–αMSH, which contains a disulfide bridge between Cys^4 and Cys^{10} amino acids [25]. Another very potent peptide agonist, also used in the characterization of melanocortin receptors, is the cyclic lactam analog melanotan II (MT-II; Table 1) [25].

For potential medical application, some linear α-MSH analogs have been labeled with the radiometals ^{111}In, ^{67}Ga, ^{64}Cu, and ^{99m}Tc via an indirect approach using 1,4,7,10-tetraazacyclododecane-*N*,*N*′,*N*″,*N*‴-tetracetic acid (DOTA) or a pyrazolyl-containing ligand as bifunctional chelators [7–9, 19, 20]. To take advantage of the superior biological properties presented by the cyclic peptides, a new family of Re- and Tc-based cyclic α-MSH analogs, MO[Cys^{3,4,10}, DPhe^7]–α-MSH$_{3–13}$ [M-CCMSH] (M is Re, ^{99m}Tc) has been developed for melanoma targeting [10, 16, 17]. The biological evaluation of the cyclic radioanalogs, ^{99m}Tc-CCMSH and ^{111}In-DOTA-ReCCMSH, has shown a significant tumor uptake but also a high kidney accumulation. Substitution of Lys^{11} by Arg^{11} led to the radioanalogs ^{99m}Tc-CCMSH(Arg^{11}) and ^{111}In-DOTA-ReCCMSH(Arg^{11}), which have shown higher tumor uptake and lower kidney accumulation, potentially interesting imaging probes for primary and pulmonary metastatic melanoma detection [11, 18]. These analogs were also labeled with therapeutic radionuclides (^{188}Re and ^{212}Pb) and their tumor uptake and therapeutic efficacy were evaluated in melanoma models [12, 13, 21, 22]. For PET imaging of melanoma the cyclic ReCCMSH(Arg^{11}) peptide was labeled with ^{64}Cu, using DOTA and a cross-bridged cyclam (CBTE2A) as bifunctional chelators [15, 23].

These results taken together showed that metal-based cyclization improves the biological behavior of the radiolabeled α-MSH analogs. Furthermore, the high MC1R affinity, stability, and prolonged activity of the cyclic MT-II agonist prompted us to explore the ^{99m}Tc(CO)$_3$-labeling and evaluation of the biological properties of an analog of MT-II, the cyclic peptide βAla-Nle-*cyclo*[Asp-His-DPhe-Arg-Trp-Lys]–NH$_2$, as well as the advantages of the lactam-based cyclization by comparison with the corresponding linear peptide.

Thus, in this paper, we report on the synthesis and characterization of the cyclic (pz-βAla-Nle-*cyclo*[Asp-His-D-Phe-Arg-Trp-Lys]-NH$_2$) and linear (pz-βAla-Nle-Asp-His-D-Phe-Arg-Trp-Lys-NH$_2$) peptide conjugates, as well as on their radiolabeling with the *fac*-[^{99m}Tc(CO)$_3$]$^+$ core, a quite versatile synthon for labeling different types of bioactive molecules, including peptides [20, 26–34]. The bifunctional chelating agent used for metal stabilization

Table 1 Structure of α-melanocyte stimulating hormone (α-MSH) and some α-MSH analogs

Bold: amino acids residues replaced in different analogs relatively to the endogeneous peptide (αMSH); underline: minimal sequence for biological activity

Peptide	No. of amino acids
Ac-Ser-Tyr-Ser-Met^4-Glu^5-His-Phe^7-Arg-Trp-Gly-Lys-Pro-Val-NH_2 (α-MSH)	13
Ac-Ser-Tyr-Ser-**Nle**^{4}-Glu^5-His-D**Phe**^{7}-Arg-Trp-Gly-Lys-Pro-Val-NH_2 (NDP-MSH)	13
Ac-**Cys**^{3}-**Cys**^{4}-Glu^5-His-D**Phe**^{7}-Arg-Trp-**Cys**^{10}-Lys-Pro-Val-NH_2 (CCMSH)	11
Ac-**Cys**^{3}-**Cys**^{4}-Glu^5-His-D**Phe**^{7}-Arg-Trp-**Cys**^{10}-Arg^{11}-Pro-Val-NH_2 [CCMSH(Arg^{11})]	11
Ac-**Nle**^{4}-***cyclo*[Asp**^{5}-His-D**Phe**^{7}-Arg-Trp-**Lys**^{10}]-NH_2 (MT-II)	7
βAla^3-**Nle**^{4}-***cyclo*[Asp**^{5}-His-D**Phe**^{7}-Arg-Trp-**Lys**^{10}]-NH_2 (**1**)	8
βAla^3-**Nle**^{4}-**Asp**^{5}-His-D**Phe**^{7}-Arg-Trp-**Lys**^{10}-NH_2 (**2**)	8

(pz) was a tridentate ligand containing a pyrazolyl-diamine backbone, which has been used with success in the radiolabeling of several other peptides, including the α-MSH analog [Ac–Nle^4,Asp^5,DPhe^7]–αMSH$_{4–11}$ (NAPamide) [20, 31–34]. We also describe the in vitro/in vivo stability studies, internalization/externalization in B16F1 cells, and biodistribution in murine melanoma-bearing mice of the radiolabeled conjugates. The advantages of using ^{99m}Tc(CO)$_3$-labeled cyclic analogs over the corresponding linear analogs for melanoma targeting are discussed.

Materials and methods

Materials

NDP-MSH was purchased from Neosystem (Strasbourg, France). Bovine serum albumin (BSA) was purchased from Sigma. Dulbecco's modified Eagle's medium (DMEM) containing GlutaMax I, fetal bovine serum, penicillin/streptomycin antibiotic solution, trypsin–EDTA, and phosphate-buffered saline (PBS) pH 7.2 were all from Gibco–Invitrogen (Alfagene, Lisbon).

Pyrazolyl-peptide conjugates: synthesis and characterization

The *tert*-butoxycarbonyl (Boc) protected pyrazolyl ligand (Me$_2$pzN[(CH$_2$)$_3$COOH]NH-Boc or Boc-pz) was prepared as previously described [31, 32]. The linear conjugate pz-βAla-Nle-Asp-His-DPhe-Arg-Trp-Lys-NH_2 was prepared by 9-fluorenylmethoxycarbonyl (Fmoc)/*t*-Bu solid-phase peptide synthesis on a Rink amide resin using the appropriate N^{α}-Fmoc-protected amino acids and *O*-(benzotriazol-1-yl)-*N*,*N*,*N*′,*N*′-tetramethyluronium tetrafluoroborate (TBTU) as a coupling agent [35, 36]. Boc-pz was incorporated on-resin to the N-terminus after assembly of the amino acid sequence. The conjugate, pz-βAla-Nle-Asp-His-DPhe-Arg-Trp-Lys-NH_2, was cleaved from the resin by acidolytic treatment with a cocktail having 95% trifluoroacetic acid (TFA) and appropriate scavengers (e.g., triethylsilane) to capture any reactive undesired species formed. The Boc group was also removed in the acidolysis.

The cyclic conjugate pz-βAla-Nle-*cyclo*[Asp-His-DPhe-Arg-Trp-Lys]-NH_2 was also prepared by standard Fmoc/^{t}-Bu solid-phase peptide synthesis using the specially protected Fmoc-Asp(ODmab)-OH and Fmoc-Lys(ivDde)-OH amino acid derivatives in order to allow on-resin cyclization prior to cleavage and full deprotection of the final peptide [37–39]. Briefly, the linear peptide sequence was normally assembled on a Fmoc–Rink–MBHA resin (0.30 mmol/g) up until the incorporation of Fmoc-Asp(ODmab)-OH, using TBTU as a coupling agent and 20% piperidine in dimethlyformamide for Fmoc-removal cycles [37]. Once Fmoc-Asp(ODmab) had been quantitatively incorporated in the peptidyl resin, this was treated with a freshly prepared mixture of hydroxylamine hydrochloride and imidazole in *N*-methylpyrrolidone to accomplish the selective and simultaneous removal of the ODmab and ivDde side chain protecting groups [40] (P. Gomes et al., unpublished results). Condensation of the Asp and Lys side chains to form the intramolecular lactam bridge was carried out using (benzotriazol-1-yloxy)tripyrrolidinophosphonium hexafluorophosphate (6 equiv), diisopropylethylamine (12 equiv), and 1-hydroxybenzotriazole (6 equiv) [37]. After lactamization had reached completion, normal assembly of the remaining peptide chain was resumed up to the quantitative incorporation of the N-terminal Boc-pz ligand. Full deprotection and cleavage of the final peptide from the solid support was performed by treatment of the peptidyl resin with TFA containing 2.5% H_2O and 2.5% triisopropylsilane. The crude product was purified by semipreparative reversed-phase (RP) high-performance liquid chromatography (HPLC) (better than 97%) and successfully characterized as the target peptide by amino acid analysis and electrospray ionization mass spectrometry (ESI–MS). Linear conjugate—calcd *m*/*z* for $[M]^+$: 1,320.76; found: 1,321.6 $[M + H]^+$. Cyclic conjugate—calcd *m*/*z* for $[M]^+$ 1,302.75; found: 1,303.87 $[M + H]^+$.

Radiolabeling

Na[$^{99m}TcO_4$] was eluted from a $^{99}Mo/^{99m}Tc$ generator, using 0.9% saline. The preparation of *fac*-[$^{99m}Tc(CO)_3(H_2O)_3]^+$ was done according to a previously described procedure, using an Isolink® kit (Mallinckrodt) [31, 32]. In a nitrogen-purged glass vial, 100 μL of a 6×10^{-4} M solution of the conjugate pz–αMSH analog was added to 900 μL of a solution of *fac*-[$^{99m}Tc(CO)_3(H_2O)_3]^+$ (37–74 MBq) in PBS. The reaction mixture was incubated at 90 or 100 °C for 50 or 60 min, for the cyclic and linear conjugates respectively, and then analyzed by RP-HPLC, using an analytical C-18 RP column. The radiolabeled compound was purified by semi-preparative RP-HPLC. The activity corresponding to the $^{99m}Tc(CO)_3$-conjugate was collected in a 50 mL Falcon flask containing 200 μL of PBS with 0.2% BSA or modified Eagle's medium (MEM) with 0.2% BSA, for biodistribution or internalization studies, respectively. The solutions were concentrated to a final volume of 200 μL under a nitrogen stream, and the product was checked by thin-layer chromatography and HPLC (see in vitro stability), to confirm its purity and stability after purification and evaporation.

HPLC analysis

RP-HPLC was performed using a PerkinElmer system (LC-Pump, series 200) coupled to a UV–vis detector (LC 290, PerkinElmer or SDP-10AV, Shimadzu) and a γ-detector (LB 507 or LB 509, Berthold) for the ^{99m}Tc compounds. Analytical separations were achieved on a Hypersil ODS column (250 mm × 4 mm, 10 μm). Semipreparative separations of the radioactive complexes were achieved on a Hypersil ODS column (250 mm × 8 mm, 10 μm). The contents of the columns were eluted with a binary gradient system with a flow rate of 1.0 mL/min (analytical), 2.0 mL/min (semipreparative for the linear radioconjugate) or 3.0 mL/min (semipreparative for the cyclic radioconjugate). Mobile phase A was 0.5% TFA and mobile phase B was CH_3CN, 0.5% TFA. The method for the analytical control of the radioconjugates was as follows: 0–18 min, 15–100% mobile phase B; 18–20 min, 100–15% mobile phase B; 20–30 min, 15% mobile phase B. The method for semipreparative separation of the linear radioconjugate was as follows: 0–3 min, 0% mobile phase B; 3–3.1 min, 0–25% mobile phase B; 3.1–9 min, 25% mobile phase B; 9–9.1 min, 25–34% mobile phase B; 9.1–14.1 min, 34–100% mobile phase B; 14.1–19 min, 100% mobile phase B; 19–21 min, 100–0% mobile phase B. The method for the semipreparative separation of the cyclic radioconjugate was as follows: 0–15 min, 15–30% mobile phase B; 15–30 min, 30% mobile phase B; 30–45 min 30–60% mobile phase B, 45–60 min 60% mobile phase B.

Thin-layer chromatography analysis

Thin-layer chromatography (TLC) was performed using silica gel TLC strips (Polygram Sil G, Macherey–Nagel) developed with a mobile phase of 5% 6 N HCl in methanol. Radioactive distribution on the TLC strips was detected using a Berthold LB 505 detector coupled to a radiochromatogram scanner.

Partition coefficient

The lipophilicity of the radioconjugates was evaluated by the "shakeflask" method [41]. The radioconjugates were added to a mixture of octanol (1 mL) and 0.1 M PBS pH 7.4 (1 mL), previously saturated in each other by stirring the mixture (1 min). This mixture was vortexed and centrifuged (3,000 rpm, 10 min, room temperature) to allow phase separation. Aliquots of both octanol and PBS were counted using a γ-counter. The partition coefficient ($P_{o/w}$) was calculated by dividing the counts in the octanol phase by those in the buffer, and the results were expressed as log $P_{o/w}$.

In vitro stability

The in vitro stability of the radioconjugates was determined in fresh human plasma. The radioconjugates (100 μL, approximately 10 MBq) were added to fresh human plasma (1 mL), and the mixtures were incubated at 37 °C. At appropriate time points (5 min, 45 min, and 4 h), 100 μL aliquots (in duplicate) were sampled and treated with 200 μL of ethanol to precipitate the proteins. Samples were centrifuged at 3,000 rpm for 15 min at 4 °C. The supernatant was analyzed by HPLC. The stability of the radiolabeled conjugates in the solutions containing 0.2% BSA was checked by HPLC (column, Supelguard LC 3 DP 2 cm × 4.6-mm inner diameter; eluents, A—10% 2-propanol and 90% 0.1% TFA, B—90% 2-propanol and 10% 0.1% TFA ; flux, 1 mL/min) and TLC (5% 6 N HCl/MeOH).

Cell culture

B16F1 murine melanoma cells (ECACC, UK) were grown in DMEM containing GlutaMax I supplemented with 10% heat-inactivated fetal bovine serum and 1% penicillin/streptomycin antibitiotic solution (all from Gibco, Alfagene, Lisbon). Cells were cultured in a humidified atmosphere of 95% air and 5% CO_2 at 37 °C (Heraeus, Germany), with the medium changed every other day. The cells were adherent in monolayers and, when confluent,

were harvested from the cell culture flasks with trypsin–EDTA (Gibco, Alfagene, Lisbon) and seeded farther apart.

Internalization and cellular retention studies

Internalization assays of the radioconjugates were performed in B16F1 murine melanoma cells seeded at a density of 0.2 million per well in 24-well tissue culture plates and allowed to attach overnight. The cells were incubated at room temperature or 37 °C for a period of 5 min to 6 h with about 200,000 cpm of the conjugate in 0.5 mL of assay medium [MEM with 25 mM *N*-(2-hydroxyethyl)piperazine-*N*′-ethanesulfonic acid and 0.2% BSA]. Incubation was terminated by washing the cells with ice-cold assay medium. Cell-surface-bound radioligand was removed by two steps of acid wash (50 mM glycine, HCl/100 mM NaCl, pH 2.8) at room temperature for 5 min. The pH was neutralized with cold PBS with 0.2% BSA, and subsequently the cells were lysed by 10 min incubation with 1 N NaOH at 37 °C to determine internalized radioligand. The cellular retention properties of the internalized radioconjugates were determined by incubating B16F1 cells with the radiolabeled compound for 3 h at 37 °C, washing them with cold assay medium, removing the membrane-bound radioactivity with acid buffer wash, and monitoring radioactivity release into the culture media (0.5 mL) at 37 °C. At different time points over a 5 h incubation period, the radioactivity in the medium and that in the cells were separately collected and counted.

Biodistribution

All animal experiments were performed in compliance with Portuguese regulations for animal treatment. The animals were housed in a temperature- and humidity-controlled room with a 12 h light/12 h dark schedule. Biodistribution of the radioconjugates was estimated in healthy and melanoma-bearing C57BL/6 female mice (8–10 weeks old). Mice were previously implanted subcutaneously with 1×10^6 B16F1 cells to generate a primary skin melanoma. Ten to 12 days after the inoculation, tumors reached a weight of 0.2–1 g.

Animals were intravenously injected into the retroorbital sinus with the radiolabeled complex (3–10 MBq) diluted in 100 μL of PBS pH 7.2. For confirming the specific uptake, 10 μg of NDP-MSH was coinjected with the radioactive complex. The effect of L-Lys coinjection on nonspecific kidney uptake of the peptide was examined in healthy C57BL/6 female mice. The animals were injected with a mixture of 3 MBq of cyclic labeled conjugate with 15 mg of L-Lys.

Mice were killed by cervical dislocation at 1, 4, and 24 h after injection. The dose administered and the radioactivity in the killed animals were measured using a dose calibrator (Curiemeter IGC-3, Aloka, Tokyo, Japan or Carpintec CRC-15W, Ramsey, USA). The difference between the radioactivity in the injected and that in the killed animals was assumed to be due to excretion. Tumors and normal tissues of interest were dissected, rinsed to remove excess blood, weighed, and their radioactivity was measured using a γ-counter (LB2111, Berthold, Germany). The uptake in the tumor and healthy tissues of interest was calculated and expressed as a percentage of the injected radioactivity dose per gram of tissue. For blood, bone, muscle, and skin, total activity was estimated assuming that these organs constitute 6, 10, 40, and 15% of the total body weight, respectively. Urine was also collected and pooled together at the time the animals were killed.

In vivo stability

The stability of the complexes was assessed by urine, and murine serum RP-HPLC analysis, under identical conditions to those used for analyzing the original radiolabeled complexes. The samples were taken 1 h after injection. The urine collected at the time the mice were killed was filtered through a Millex GV filter (0.22 μm) before RP-HPLC analysis. Blood collected from the mice was centrifuged at 3,000 rpm for 15 min at 4 °C, and the serum was separated. The serum was treated with ethanol in a 2:1 (v/v) ratio to precipitate the proteins. After centrifugation at 3,000 rpm for 15 min at 4 °C, the supernatant was collected and analyzed by RP-HPLC.

Results and discussion

The presence of α-MSH receptors on melanoma cells and the fact that the receptors undergo rapid internalization on ligand binding have led researchers to explore the possibility of using radiolabeled α-MSH analogs for melanoma diagnosis or therapy. Encouraging data on the use of cyclic Re-CCMSH peptides and peptide labeling with the *fac*-$[^{99m}Tc(CO)_3]^+$ moiety through the bifunctional chelating approach led us to consider the possibility of developing a new class of melanoma-specific $^{99m}Tc(CO_3)$-labeled α-MSH analogs based on the MT-II peptide (Table 1) [25]. MT-II is a 23-membered ring formed from lactam cyclization through the Lys and Asp side chains. The bioactive conformation of MT-II involves a stable type 2 β-turn around the core His-DPhe-Arg-Trp region, compared with the type 3 β-turn of its linear analog, and the three hydrophobic aromatic rings in a stacked orientation

opposite the hydrophilic side chain of Arg [25]. As a consequence, MT-II has a high affinity for melanocortin receptors.

Investigations on the effects of modifications at the N-terminal of MT-II and His-DPhe-Arg-Trp-NH_2 peptides on ligand potency [25] led us to believe that the affinity of MT-II for the MC1 receptor would not be negatively influenced by insertion of a βAla spacer and attachment of a pz chelator to the N-terminus, yielding the cyclic conjugate pz-βAla-Nle-*cyclo*[Asp-DPhe-Arg-Trp-Lys]-NH_2 (Scheme 1). To evaluate the advantages of lactam cyclization in the pharmacokinetic profile and tumor-targeting properties of the radioconjugates we also prepared and assessed the biological properties of the respective linear radioconjugate.

The cyclic and linear pz–peptide conjugates were prepared by standard solid-phase synthetic methods, purified by preparative RP-HPLC (purity 97% or better), and characterized by ESI–MS (m/z = 1,303.87 and 1,321.6 $[M + H]^+$ for the cyclic and the linear conjugate, respectively).

The radioconjugates containing the linear peptide ([^{99m}Tc(CO)$_3$-pz-βAla-Nle-Asp-DPhe-Arg-Trp-Lys-NH_2]) and the cyclic peptide ([^{99m}Tc(CO)$_3$-pz-βAla-Nle-*cyclo*[Asp-DPhe-Arg-Trp-Lys]-NH_2]) were prepared by reaction of the precursor *fac*-[^{99m}Tc(CO)$_3$(H$_2$O)$_3$]$^+$ (prepared via an Isolink® kit) with the conjugates at 90–100 °C, for 50–60 min (Scheme 1).

After optimization of the labeling conditions, namely, temperature and reaction time, radiochemical yields higher than 95% were obtained for both complexes using a final concentration of conjugate of 6×10^{-5} M. The RP-HPLC analytical retention times were 11.7 and 10.8 min for the ^{99m}Tc(CO)$_3$-labeled cyclic and linear conjugates, respectively.

In order to increase specific activity and to maximize cellular and tumor uptake, the ^{99m}Tc(CO)$_3$-labeled conjugates were separated from the corresponding nonmetallated conjugates by semipreparative RP-HPLC. The fraction corresponding to each radioconjugate was collected in a 50 mL Falcon vial containing PBS or MEM solutions with 0.2% BSA (for biodistribution or internalization studies, respectively), to avoid adsorption phenomena, after evaporation of the HPLC elution solvent (CH_3CN). The stability of the radioconjugates in PBS and MEM solutions was evaluated by HPLC and TLC, and it was found that no interaction with BSA and/or transmetallation took place under those conditions. Indeed, the HPLC chromatogram (Supelguard LC 3 DP 2 cm × 4.6 mm inner diameter column) of the cyclic radioconjugate, after 4 h incubation at 37 °C in a 0.2% BSA solution in PBS, displays only the radioconjugate (γ-detection; retention time, 6.0 min) and BSA (UV detection; retention time, 9.8 min). Furthermore, on analyzing the TLC radiochromatogram of the cyclic radioconjugate after 24 h incubation at 37 °C in a 0.2% BSA solution in MEM, we detected no hydrolyzed ^{99m}Tc species ($R_f = 0$), labeled BSA ($R_f = 0$), [^{99m}TcO$_4$]$^-$ ($R_f = 0.85$), or *fac*-[^{99m}Tc(CO)$_3$(H$_2$O)$_3$] precursor (R_f = 0.80), and the radiolabeled cyclic conjugate was the only radiochemical species present ($R_f = 0.44$). A similar stability profile has been observed for the ^{99m}Tc(CO)$_3$-labeled linear conjugate. The results obtained with HPLC and TLC

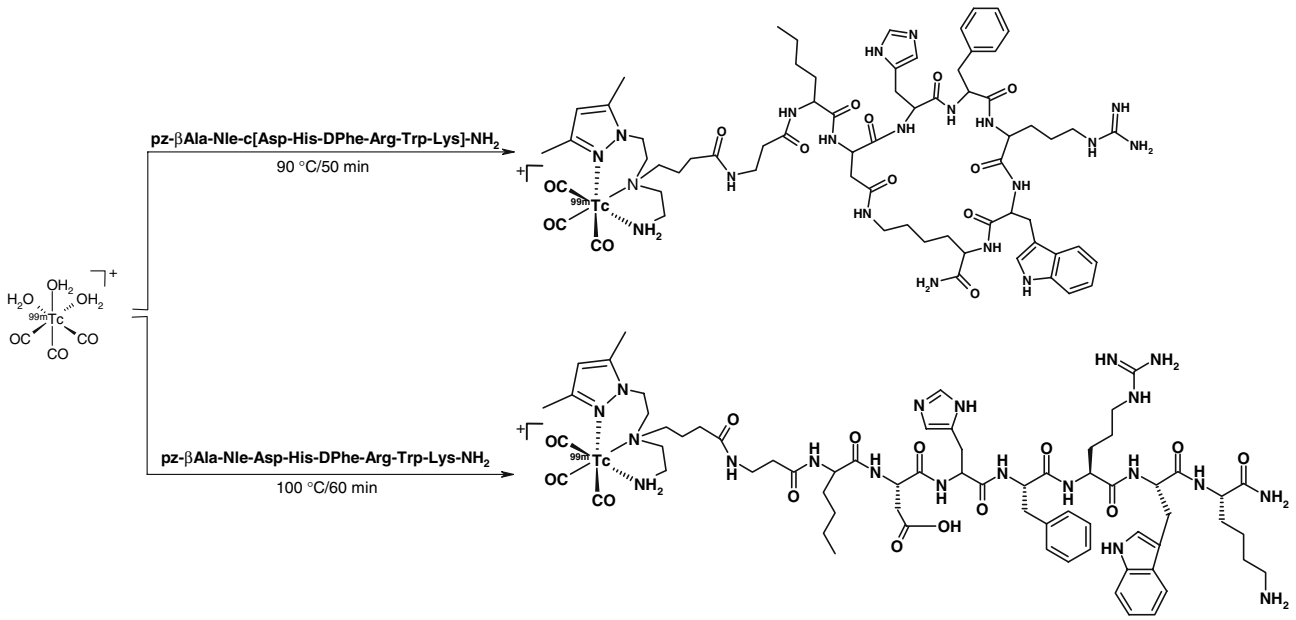

Scheme 1 Synthesis of the radioconjugates [^{99m}Tc(CO)$_3$-pz-βAla-Nle-*cyclo*[Asp-DPhe-Arg-Trp-Lys]-NH_2] and [^{99m}Tc(CO)$_3$-pz-βAla-Nle-Asp-DPhe-Arg-Trp-Lys-NH_2]

indicate that both the linear and the cyclic radiopeptide were stable in the presence of BSA and MEM, and confirm the high ability of the pyrazolyl-diamine chelator to stabilize the *fac*-[^{99m}Tc(CO)$_3$]$^+$ moiety, avoiding transmetallation and/or reoxidation of the ^{99m}Tc(I) [31–34].

To assess the resistance of the radioconjugate to proteolytic degradation caused by endogenous peptidases and to predict its in vivo stability, we performed stability assays in fresh human plasma at 37 °C. Analysis by RP-HPLC at different incubation time points (0 min, 5 min, 45 min, and 4 h) indicated high plasma stability with negligible degradation of both the linear and the cyclic radioconjugates, and a purity of 98% or better. Again, it has been shown that the pyrazolyl-diamine chelating unit is able to stabilize the metal center against transmetallation reactions to serum-based proteins.

The lipophilicity of both radiopeptides was evaluated by determination of the partition coefficient in physiological conditions. While the cyclic radioconjugate was moderately hydrophobic (log $P_{o/w} = 0.196 \pm 0.003$), the linear analog revealed a hydrophilic character (log $P_{o/w} = -1.074 \pm 0.010$).

The degree of internalization in B16F1 murine melanoma cells is a very important parameter for predicting tumor-targeting properties of the labeled peptides. Internalization studies performed for both radioconjugates, at room temperature and at 37 °C, revealed that the cellular uptake was temperature-dependent and time-dependent (Fig. 1).

As shown in Fig. 1, higher levels of internalization were reached for the ^{99m}Tc(CO)$_3$-labeled cyclic conjugate, compared with the linear one. For instance, at 4 h after incubation (37 °C), while only approximately 30% of the total cell-associated activity for the administered linear radioconjugate was taken up and internalized by the cells, 79% was internalized for the cyclic radiopeptide (Fig. 1, panels A, B). A striking difference between the levels of internalization is observed when this parameter is expressed as a percentage of total activity (Fig. 1, panel C). In fact, while a negligible amount of radioactivity (1.6%) was internalized after 4 h for the linear radiopeptide, a remarkable internalization (41.8 and 50.5% for 4 and 6 h, respectively) was attained for the cyclic radioconjugate. These values are particularly high when compared with data previously reported for other radiolabeled α-MSH analogs. Indeed, for ^{64}Cu-DOTA-NAPamide and ^{99m}Tc(CO)$_3$-pz-NAPamide the maximum internalization observed was approximately 4.5% of the applied activity 3 h after incubation [9, 20]. In the case of the cyclic radiopeptide ^{99m}Tc-CCMSH, using the same experimental conditions as those used for the ^{99m}Tc(CO)$_3$-labeled cyclic conjugate (0.2×10^6 melanoma B16F1 cells per well and 200,000 cpm of radioconjugate per well), the maximum internalization achieved was less than 4% [17].

The cellular retention of the radioconjugates was also evaluated in B16F1 cells at different time points (Fig. 2). A moderate retention was observed for the linear radioconjugate, with 35.3% of the cell-associated activity still remaining inside the cells after 4 h. In the case of the cyclic radioconjugate, a remarkably higher degree of cellular retention was observed. Indeed, the ^{99m}Tc(CO)$_3$-labeled cyclic conjugate was slowly released from the cells into the medium, with about 75% of the radioactivity still associated with the cells even after 5 h incubation. The enhanced internalization and intracellular retention of the cyclic radioconjugate, compared with that of its linear counterpart, is much likely related with the compact structure of the former. In fact, this structure seems to confer a more potent agonistic binding behavior to the peptide and an increased resistance to proteolysis.

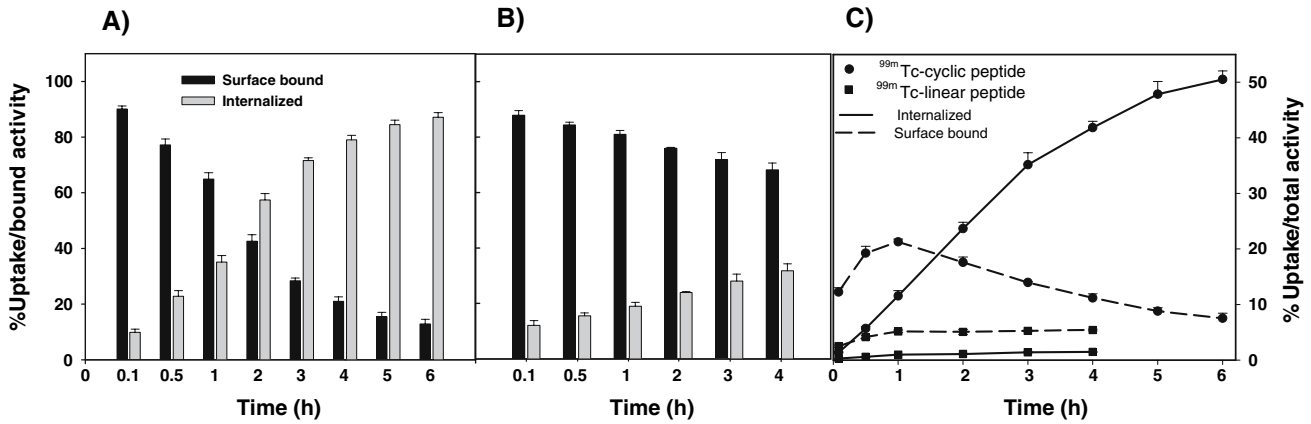

Fig. 1 Internalization of the radioconjugates in B16F1 cells at different time points (37 °C). Internalized and surface-bound activity expressed as a fraction of bound activity (activity on the membrane surface and inside the cell) for the cyclic radioconjugate (*A*) and the linear radioconjugate (*B*); internalized and surface-bound activity expressed as a percentage of total activity for both radioconjugates (*C*)

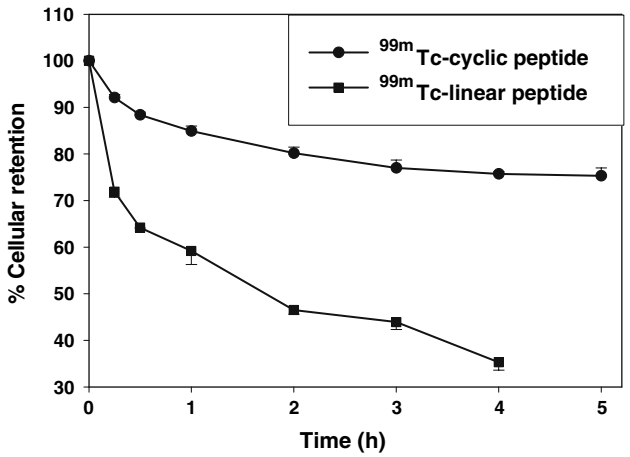

Fig. 2 Cellular retention of internalized linear and cyclic radioconjugates in B16F1 cells over time at 37 °C

The biodistribution of $^{99m}Tc(CO)_3$-labeled α-MSH analogs was examined in a B16F1 melanoma-bearing mouse model, at 1, 4, and 24 h after intravenous injection. Biodistribution data for the linear and the cyclic radioconjugate are presented in Tables 2 and 3, respectively.

Biodistribution data from the linear radioconjugate indicate a fast clearance from the bloodstream [0.40 ± 0.05% injected dose (ID)/g, 4 h after injection] and other main organs, including skeletal and soft tissues like muscle. The overall radioactivity elimination occurs mainly by the urinary excretion route as indicated by the percentage of total excretion (56.4% at 1 h after injection), which predominantly corresponds to urine. Nevertheless, a significant portion of radioactivity is rapidly taken up by the liver and cleared into intestines, suggesting the importance of the hepatobiliary excretion pathway (11.7 ± 2.6 and 18.4 ± 3.1% ID per organ at 1 h after injection; 2.1 ± 0.8 and 26.8 ± 2.4% ID per organ at 4 h after injection, for liver and intestine, respectively).

The effect of cyclization on the biodistribution profile of the radioconjugate was mainly reflected in the decrease of clearance from most organs and in the radioactivity retained in the excretory organs, like liver and kidney. As a consequence of this behavior, the overall excretion from the whole animal body was significantly low. Indeed, 1 h after injection only 14.2% of the total activity was eliminated and 67% of that activity still remained in the animal 4 h after injection.

Owing to the high liver mass, the uptake for the cyclic analog in this organ was relatively high (23.5 ± 1.3% ID per organ, 4 h after injection), when compared with the kidney uptake (9.2 ± 0.7% ID per organ, 4 h after injection). Nevertheless, this result could be predicted from the lipophilic character (log $P_{o/w}$ = 0.196 ± 0.003) presented by the cyclic radioconjugate. A shift from the hepatobiliary

Table 2 Biodistribution of the $^{99m}Tc(CO)_3$-labeled linear conjugate in B16F1 murine melanoma-bearing C57BL/6 mice at 1, 4, and 24 h after intravenous injection (mean ± standard deviation, n = 4–5)

Tissue/organ	Percentage ID/g ± standard deviation			
	1 h	4 h	4 h with NDP[a]	24 h
Tumor	1.96 ± 0.17	0.99 ± 0.08	0.55 ± 0.11	0.027 ± 0.010
Blood	1.08 ± 0.28	0.40 ± 0.05	0.37 ± 0.06	0.011 ± 0.002
Liver	11.28 ± 1.28	2.02 ± 0.82	1.36 ± 0.39	0.033 ± 0.002
Intestine	10.37 ± 2.36	16.18 ± 3.75	19.70 ± 2.29	0.056 ± 0.048
Spleen	1.42 ± 0.11	0.30 ± 0.05	0.31 ± 0.08	0.018 ± 0.004
Heart	0.35 ± 0.01	0.11 ± 0.02	0.10 ± 0.02	0.004 ± 0.001
Lung	1.14 ± 0.13	0.34 ± 0.09	0.44 ± 0.10	0.012 ± 0.002
Kidney	7.77 ± 0.57	1.64 ± 0.19	1.59 ± 0.21	0.029 ± 0.001
Muscle	0.25 ± 0.12	0.10 ± 0.06	0.03 ± 0.01	0.002 ± 0.001
Bone	0.36 ± 0.05	0.08 ± 0.02	0.07 ± 0.01	0.003 ± 0.001
Stomach	2.17 ± 1.45	0.73 ± 0.50	0.47 ± 0.26	0.031 ± 0.022
Adrenals	1.10 ± 0.07	0.32 ± 0.20	0.38 ± 0.11	0.012 ± 0.001
Pancreas	0.25 ± 0.05	0.16 ± 0.08	0.44 ± 0.19	0.002 ± 0.000
Skin	0.38 ± 0.03	0.08 ± 0.03	0.08 ± 0.03	0.002 ± 0.001
Uptake ratio of tumor to normal tissue				
Tumor/blood	1.8	2.5	1.5	2.4
Tumor/muscle	7.8	9.9	18.3	13.5
Total excretion (%)	56.4 ± 5.8	64.4 ± 4.3	63.6 ± 3.4	96.0 ± 2.6

ID injected dose, *NDP* (Nle^4,DPhe^7)-αMSH

[a] Coinjection of the radioconjugate with NDP

Table 3 Biodistribution of the $^{99m}Tc(CO)_3$-labeled cyclic conjugate in B16F1 murine melanoma-bearing C57BL/6 mice at 1, 4, and 24 h after intravenous injection (mean ± standard deviation, $n = 4–5$)

Tissue/organ	Percentage ID/g ± standard deviation			
	1 h	4 h	4 h with NDP[a]	24 h
Tumor	9.26 ± 0.83	11.31 ± 1.83	2.97 ± 0.62	3.48 ± 0.40
Blood	2.71 ± 0.64	1.67 ± 0.24	1.46 ± 0.13	0.20 ± 0.05
Liver	42.19 ± 5.05	22.86 ± 1.17	24.69 ± 3.16	1.72 ± 0.12
Intestine	5.17 ± 0.91	8.45 ± 0.76	11.00 ± 1.04	1.15 ± 0.37
Spleen	2.54 ± 0.28	2.24 ± 0.37	1.86 ± 0.37	0.46 ± 0.09
Heart	1.04 ± 0.19	0.48 ± 0.07	0.44 ± 0.05	0.15 ± 0.01
Lung	3.85 ± 0.46	1.54 ± 0.16	1.72 ± 0.32	0.90 ± 0.52
Kidney	71.06 ± 6.44	32.12 ± 1.57	42.37 ± 3.07	1.48 ± 0.24
Muscle	0.35 ± 0.07	0.19 ± 0.08	0.18 ± 0.06	0.03 ± 0.00
Bone	1.14 ± 0.19	0.70 ± 0.13	0.48 ± 0.04	0.09 ± 0.01
Stomach	1.97 ± 0.75	0.88 ± 0.46	0.93 ± 0.27	0.25 ± 0.30
Pancreas	0.73 ± 0.32	0.39 ± 0.10	0.26 ± 0.04	0.07 ± 0.01
Skin	0.84 ± 0.12	0.53 ± 0.10	0.57 ± 0.10	0.13 ± 0.08
Uptake ratio of tumor to normal tissue				
Tumor/blood	3.4	6.8	2.0	17.4
Tumor/muscle	26.5	61.4	16.5	116
Total excretion (%)	14.2 ± 2.3	37.4 ± 2.4	33.0 ± 1.5	87.6 ± 3.2

[a] Coinjection of the radioconjugate with NDP

towards the renal excretion pathway could be achieved by reducing the lipophilicity of the radiopeptide by introducing Asp or Glu residues (polar, negatively charged, and very hydrophilic amino acids) in the peptide sequence. No significant uptake or retention of radioactivity in the stomach was observed for both radioconjugates, indicating minimal, if any, in vivo oxidation of the complexes to $[^{99m}TcO_4]^-$.

The most striking difference between the two $^{99m}Tc(CO)_3$-labeled conjugates is related to tumor uptake. While a low tumor uptake for the ^{99m}Tc-labeled linear peptide was found (1.96 ± 0.17 and 0.99 ± 0.08% ID/g at 1 and 4 h after injection, respectively), a fast and remarkable activity accumulation in the MC1R-expressing B16F1 tumor was observed for the cyclic radioconjugate. Indeed, 1 h after injection, a tumor uptake of 9.26 ± 0.83% ID/g was found, with this value increasing slowly to 11.31 ± 1.83% ID/g at 4 h after injection. The activity was then slowly washed out from the tumor, and the uptake dropped to a still relevant value of 3.48 ± 0.40% ID/g over 24 h. The high tumor uptake and the high tumor retention are in agreement with the high internalization and slow washout observed in in vitro studies with B16F1 cells for the cyclic radioconjugate, reflecting again the advantages of lactam cyclization in MC1R affinity and potency and in resistance to intracellular degradation.

The in vivo specificity of the radioconjugates for the MC1R was evaluated by their coadministration with cold NDP-MSH peptide (linear α-MSH peptide analog with picomolar affinity for the MC1R expressed on murine melanoma cells) in the same animal model. The receptor-blocking studies at 4 h after injection revealed that the tumor uptake was significantly reduced by 74.8 and 44.5% for the cyclic and linear radioconjugates, respectively, in the presence of NDP-MSH, without significant changes in the biodistribution profile of the radioconjugates in healthy tissues (Tables 2, 3). These results confirmed that tumor uptake of both radioconjugates is MC1R-mediated, and that both peptides kept their biological activity upon conjugation to the pz-containing chelator and consequent $^{99m}Tc(CO)_3$ labeling. Tumor-to-blood and tumor-to-muscle uptake ratios were higher for the cyclic than for the linear radioconjugate despite the slow clearance from nontarget organs. Furthermore, for the cyclic radioconjugate the tumor-to-blood and tumor-to-muscle uptake ratios increased from 6.8 and 61.4 (4 h after injection) to 17.4 and 116 (24 h after injection), which also indicates a receptor-mediated transport, and subsequent intracellular trapping of this radiocomplex in the MC1R-expressing tumor.

The high tumor uptake and retention found for the $^{99m}Tc(CO)_3$-labeled cyclic conjugate, compared with its linear counterpart, is in full agreement with the data obtained for the cyclic ^{99m}Tc/Re-CCMSH analog, using the same animal model (B16F1 melanoma-bearing C57BL/6 mice) [10, 17]. The linear, nonmetallated, ^{111}In-DOTA-

CCMSH exhibited also a lower tumor uptake than the homolog ^{111}In-DOTA-ReCCMSH (4.32 ± 0.59 vs. 9.49 ± 0.90% ID/g, 4 h after injection), clearly showing the benefit of ReO-mediated cyclization or peptide cyclization itself [10]. The best tumor uptake obtained with ^{111}In-DOTA-ReCCMSH (ReO cyclization) compared with the disulfide-bond-cyclized analog ^{111}In-DOTA-CMSH indicated that different methods of peptide cyclization yield molecules with different in vivo biodistribution properties [10]. In addition, ^{111}In-DOTA-ReCCMSH exhibited again superior tumor retention values compared with the cyclic ^{99m}Tc-CCMSH at 24 h after injection (4.86 ± 1.52 vs. 1.38 ± 0.36% ID/g), although they were not statistically different at early time points [10, 17]. Herein, we have demonstrated that the cyclization through a lactam bridge appears to be another promising method of peptide cyclization for radiolabeled α-MSH analogs.

The ^{99m}Tc(CO)$_3$-labeled linear conjugate presents a very low tumor uptake (1.96 ± 0.17 and 0.99 ± 0.08% ID/g at 1 and 4 h after injection, respectively). The same peptidic linear sequence, previously labeled with ^{111}In using the DOTA chelator, displayed also a relatively low tumor uptake without significant retention (4.31 ± 0.30 and 1.17 ± 0.13% ID/g for 4 and 24 h, respectively) [19]. These results taken together indicate that a constrained structure, conferred by lactam-based cyclization in this particular amino acid sequence, significantly favors the peptide–MC1R interaction.

However, cyclization of the linear peptide through lactam formation led to an impressive increase in kidney uptake (for the linear peptide 1.64 ± 0.19% ID/g and for the cyclic peptide 32.12 ± 0.19% ID/g, at 4 h after injection). Since it is well established that administration of cationic amino acids (Lys and Arg) inhibits renal accumulation of radiolabeled proteins and peptides [42, 43], we performed a second set of biodistribution experiments in healthy mice in which Lys was coinjected with the cyclic radioconjugate (Table 4). Interestingly, coadministration of this basic amino acid did not reduce significantly kidney accumulation of ^{99m}Tc(CO)$_3$-labeled cyclic peptide, which seems to indicate that the electrostatic interaction between the positively charged complex and the negatively charged surface of the proximal tubule cells is not a major factor for tubular reabsorption. This behavior has already been observed for similar α-MSH analogs labeled with other radiometals [M-DOTA-Re(Arg^{11})CCMSH; M is ^{90}Y, ^{177}Lu] [44]. In these studies, the multiligand megalin receptor, strongly expressed in the renal proximal tubule, was proposed as the main system involved in the renal uptake of the complexes [45, 46].

In vivo stability studies revealed that both linear and cyclic radioconjugates are stable in blood (1 h after injection), as no metabolites could be detected (Fig. 3).

Table 4 Biodistribution of the ^{99m}Tc(CO)$_3$-labeled cyclic conjugate coinjected with or without 15 mg of L-Lys in healthy C57BL/6 mice, at 1 h after intravenous injection (mean ± standard deviation, n = 4–5)

Tissue/organ	Percentage ID/g ± standard deviation	
	With L-Lys	Without L-Lys
Blood	3.03 ± 1.75	2.83 ± 1.04
Liver	28.15 ± 4.05	24.71 ± 1.94
Intestine	2.79 ± 0.72	2.70 ± 0.68
Spleen	1.87 ± 0.36	2.39 ± 0.66
Heart	0.96 ± 0.30	0.86 ± 0.14
Lung	2.67 ± 0.95	2.07 ± 1.03
Kidney	49.44 ± 5.87	59.38 ± 11.79
Muscle	0.30 ± 0.08	0.31 ± 0.05
Bone	0.75 ± 0.30	0.79 ± 0.21
Stomach	3.36 ± 1.57	4.62 ± 2.94
Adrenals	11.31 ± 8.61	4.98 ± 2.29
Pancreas	0.44 ± 0.15	0.66 ± 0.48
Skin	1.08 ± 0.15	1.15 ± 0.18
Total excretion (%)	17.0 ± 2.2	12.7 ± 2.2

The plasmatic protein-bound fraction for the radioconjugates was relatively low (21 and 22% for cyclic and linear radioconjugates, respectively). These results indicate again that metal complexation via the tridentate pyrazolyldiamine backbone overcomes potential binding/transmetallation to coordinating residues in circulating proteins,

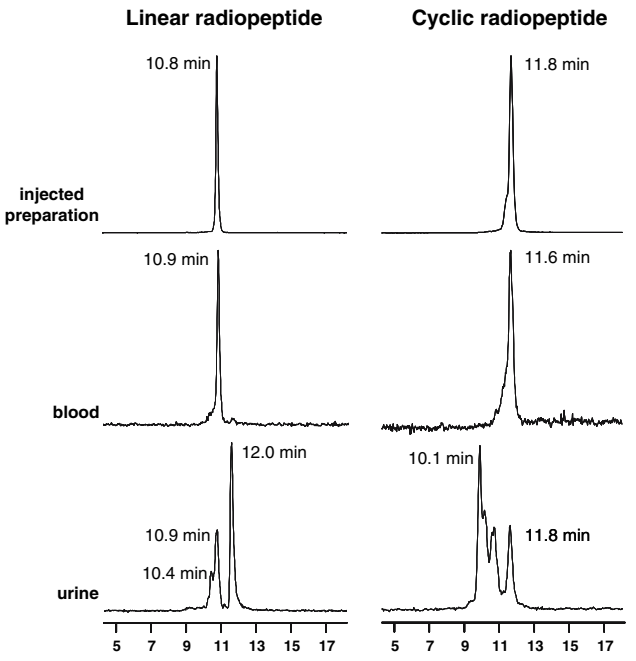

Fig. 3 Reversed-phase high-performance liquid chromatography chromatograms of the injected preparation, blood serum, and urine samples collected 1 h after injection

such as His, Cys, or Met. In contrast, metabolites from both radioconjugates were found in urine. While a more hydrophobic species was observed for the linear radioconjugate (retention time 12.0 vs. 10.9 min), the metabolites of the cyclic radioconjugate were essentially hydrophilic species with the major metabolite appearing at 10.1 min.

In conclusion, we have prepared a MT-II-based cyclic $^{99m}Tc(CO_3)$ radiopeptide and the corresponding linear analog in high yield and radiochemical purity. Both radioconjugates displayed good stability in vitro and in vivo. The cyclization through a lactam bridge resulted in a compact structure that remarkably enhanced the cellular internalization and retention, and consequently MC1R-mediated tumor uptake in B16F1 melanoma-bearing mice. Despite the promising tumor-targeting properties exhibited by the cyclic radiopeptide, its pharmacokinetic profile has still to be improved. Higher excretion and lower kidney uptake can certainly be reached either by modifying the physicochemical properties of the bifunctional chelating agent (e.g., charge and hydrophilicity) or by changing some of the amino acids of the peptide.

Acknowledgments Mallinckrodt-Tyco Inc. is acknowledged for financial support and for providing IsoLink® kits. C.X. thanks Fundação para a Ciência e Tecnologia (FCT) for a PhD grant (SFRH/BD/16680/2004). P.G. thanks FCT for pluriannual funding to the CIQ(UP) research unit.

References

1. Carlson JA, Slominski A, Linette GP, Mihm MC, Ross JS (2003) Expert Rev Mol Diagn 3:303–330
2. Mijnhout GS, Hoekstra OS, Tulder MW, Teule GJ, Deville WL (2001) Cancer 91:1530–1542
3. Dimitrakopoulou-Strauss A, Strauss LG, Burger C (2001) J Nucl Med 42:248–256
4. Ghanem GE, Comunale G, Libert A, Vercammen-Grandjean A, Lejeune FJ (1988) Int J Cancer 41:248–255
5. Siegrist W, Solca F, Stutz S, Giuffre L, Carrel S, Girard J, Eberle AN (1989) Cancer Res 49:6352–6358
6. Siegrist W, Stutz S, Eberle AN (1994) Cancer Res 54:2604–2610
7. Eberle AN, Froidevaux S (2003) J Mol Recognit 16:248–254
8. Froidevaux S, Calame-Christe M, Shuhmacker J, Tanner H, Saffrich R, Henze M, Eberle AN (2004) J Nucl Med 45:116–123
9. Cheng Z, Xiong Z, Subbarayan M, Chen X, Gambhir SS (2007) Bioconjug Chem 18:765–772
10. Chen J-Q, Cheng Z, Owen NK, Hoffman TJ, Miao Y, Jurisson SS, Quinn TP (2001) J Nucl Med 42:1847–1855
11. Cheng Z, Chen J, Miao Y, Owen NK, Quinn TP, Jurisson SS (2002) J Med Chem 45:3048–3056
12. Miao Y, Owen NK, Whitener D, Gallazzi F, Hoffman TJ, Quinn TP (2002) Int J Cancer 101:480–487
13. Miao Y, Whitener D, Feng W, Owen NK, Chen J, Quinn TP (2003) Bioconjug Chem 14:1177–1184
14. Miao Y, Hoffman TJ, Quinn TP (2005) Nucl Med Biol 32:485–493
15. Wei L, Butcher C, Miao Y, Gallazzi F, Quinn TP, Welch MJ, Lewis JS (2007) J Nucl Med 48:64–72
16. Giblin MF, Wang N, Hoffman TJ, Jurisson SS, Quinn TP (1998) Proc Natl Acad Sci USA 95:12814–12818
17. Chen J-Q, Chen Z, Hoffman TJ, Jurisson SS, Quinn TP (2000) Cancer Res 60:5649–5658
18. Miao Y, Benwell K, Quinn TP (2007) J Nucl Med 48:73–80
19. Froidevaux S, Calame-Christe M, Tanner H, Sumanovski L, Eberle AN (2002) J Nucl Med 43:1699–1706
20. Raposinho PD, Correia JDG, Alves S, Botelho MF, Santos AC, Santos I (2008) Nucl Med Biol 35:91–99
21. Miao Y, Owen NK, Fisher DR, Hoffman TJ, Quinn TP (2005) J Nucl Med 46:121–129
22. Miao Y, Hylarides M, Fisher DR, Shelton T, Moore H, Wester DW, Fritzberg AR, Winkelmann CT, Hoffman TJ, Quinn TP (2005) Clin Cancer Res 11:5616–5621
23. McQuade P, Miao Y, Yoo J, Quinn TP, Welch MJ, Lewis JS (2005) J Med Chem 48:2985–2992
24. Garcia-Borrón JC, Sánchez-Laorden BL, Jiménez-Cervantes C (2005) Pigment Cell Res 18:393–410
25. Holder JR, Haskell-Luevano C (2004) Med Res Rev 24:325–56
26. Alberto R, Pak JK, Staveren DV, Mundwiler S, Benny P (2004) Biopolymers 76:324–333
27. Alberto R (2005) Top Curr Chem 252:1–44
28. Schibli R, Schubiger AP (2002) Eur J Nucl Med 29:1529–1542
29. Santos I, Paulo A, Correia JDG (2005) Top Curr Chem 252:45–84
30. Banerjee SR, Maresca KP, Francesconi L, Valliant J, Babich JW, Zubieta J (2005) Nucl Med Biol 32:1–20
31. Alves S, Paulo A, Correia JDG, Domingos Â, Santos I (2002) J Chem Soc Dalton Trans 24:4714–4719
32. Alves S, Paulo A, Correia JDG, Gano L, Smith CJ, Hoffman TJ, Santos I (2005) Bioconjug Chem 16:438–449
33. Alves S, Correia JDG, Santos I, Veerendra B, Sieckman GL, Hoffman TJ, Rold T, Retzloff L, McCrate J, Prasanphanich A, Smith CJ (2006) Nucl Med Biol 33:625–634
34. Alves S, Correia JDG, Gano L, Rold TL, Prasanphanich A, Haubner R, Rupprich M, Alberto R, Decristoforo C, Santos I, Smith CJ (2007) Bioconjug Chem 18:530–537
35. Fields GB, Noble RL (1990) Int J Pept Protein Res 35:161–214
36. Knorr R, Trzeciak A, Bannwarth W, Gillessend D (1989) Tetrahedron Lett 30:1927–1930
37. Lloyd-Williams P, Albericio F, Giralt E (1997) Chemical approaches to the synthesis of peptides and proteins. CRC, Boca Raton
38. Chhabra SR, Hothi B, Evans D J, White PD, Bycroft BW, Chan WC (1998) Tetrahedron Lett 39:1603–1606
39. Chan WC, Bycroft BW, Evans DJ, White P D (1995) J Chem Soc Chem Commun 21:2209–2210
40. Díaz-Mochón J, Bialy L, Bradley M (2004) Org Lett 6:1127–1129
41. Troutner DE, Volkert WA, Hoffman TJ, Holmes RA (1984) Int J Appl Radiat Isot 35:10467–10470
42. Behr TM, Goldenberg DM, Becker W (1998) Eur J Nucl Med 25:201–212
43. Rolleman EJ, Valkema R, de Jong M, Kooij PPM, Krenning ER (2003) Eur J Nucl Med 30:9–15
44. Miao Y, Fisher DR, Quinn TP (2007) Nucl Med Biol 33:723–733
45. de Jong M, Barone R, Krenning E, Bernard B, Melis M, Visser T, Gekle M, Willnow TE, Walrand S, Jamar F, Pauwels S (2005) J Nucl Med 46:1696–1700
46. Verroust PJ, Christensen EI (2002) Nephrol Dial Transplant 17:1867–1871